Unified channel model for mobile radio systems with smart antennas

J. Fuhl
A.F. Molisch
E. Bonek

Indexing terms: Channel modelling, Smart antennas

Abstract: The definition of flat fading and frequency-selective fading channels is extended to low-rank and high-rank channels to include the angular domain. By physical reasoning a generic channel model is introduced incorporating directions of arrival and a set of parameters is given for its configuration. The time evolution of the scattering processes and directions of arrival is taken into account. Analytical expressions are derived for space-correlation coefficients and frequency-correlation coefficients. Spatial correlation decreases with increasing angular spread and decreasing angle of incidence, measured from array broadside.

1 Introduction

Channel modelling is an important issue for the design and analysis of mobile communication systems. Given a description of the channel, efficient signal processing schemes can be devised and system performance analysed. Most models describe received field strength, power delay profiles, and Doppler spectra; these parameters are important for the analysis of systems with omnidirectional antennas. For the design of smart antenna systems, however, we also need knowledge about directions of arrival (DOA). It is not possible to derive DOAs from conventional models. Doppler spectra are not uniquely associated with DOAs, since we would also need to know velocity and direction of motion of the mobile station (MS) and the scatterers. Thus the design of smart antenna systems requires new channel models.

In the past, several direction-dependent channel models have been proposed [1–6]. The earliest was the local scatterer model by [1]; it was intended for macrocells and suggested that all scatterers are distributed uniformly on a circle around the MS. A refinement of that model for micro- and picocells was suggested in [2, 7], allowing for scatterers both within the scattering disc (not just on a circle) and around the base station (BS). Geometrically based models, which are mainly suitable for micro- and picocells, were proposed in [4, 3]. Measurements suggest that the local scattering model is always valid for macrocells [8, 9], whereas for microcells the geometrically based model seems preferable [5].

Although these models have been valuable for attaining initial insights into the performance of smart antenna systems, they have been designed for specific situations. The present paper gives a generalised and unified model for macro-, micro- and picocells, with or without a line of sight (LOS) component, and with or without movement of the mobile station. We give the range of parameters that cover the situations typically occurring in practical situations, so that this paper contains all information required for immediate implementation. Our unified channel model has already been successfully applied for simulations of smart antenna systems [10–13].

IEE Proceedings online no. 19981750

Paper first received 22nd April and in revised form 29th October 1997

The authors are with the Institut für Nachrichtentechnik und Hochfrequenztechnik, Technische Universität Wien, Gusshausstrasse 25/389, A-1040 Wien, Austria

2 Low-rank and high-rank channel models

When the transfer function of the mobile radio channel is observed in the frequency band of interest, two different kinds of fading may appear: flat fading and frequency-selective fading. To include angular dispersion we make the following generalised definition of low-rank channel models, and high-rank channel models:

Let $\varphi_{3\text{dB}}$ denote the 3dB beamwidth of the antenna array in azimuth with equal-amplitude and equal-phase feed currents, at the BS.

Definition: A channel is *low rank* if the delay spread S_t [14] is small compared to the inverse of the receiver filter bandwidth B_{filter} and the angular spread S_φ [6] is small compared to the 3-dB beamwidth $\varphi_{3\text{dB}}$ of the antenna pattern

$$S_t \ll \frac{1}{B_{filter}} \quad \text{and} \quad S_\varphi \ll \varphi_{3\text{dB}} \tag{1}$$

A channel is *high rank* if the delay spread S_t is equal to or larger than the inverse of the receiver filter bandwidth B_{filter} or the angular spread S_φ is equal to or larger than the 3-dB beamwidth $\varphi_{3\text{dB}}$ of the antenna pattern

$$S_t \gtrsim \frac{1}{B_{filter}} \quad \text{or} \quad S_\varphi \gtrsim \varphi_{3\text{dB}} \tag{2}$$

Strictly speaking, the directional dispersion of the incident field depends on both φ and θ, the azimuth and elevation angles, respectively. To keep the number of

free parameters within reasonable limits we restrict the scope of this paper to azimuth only. Note that high-rank channels also include the purely time-dispersive channels (without angular dispersion), and the purely angular dispersive channels.

Since the angular dispersion is not the same for BS and MS, a channel may be high rank for the downlink, but low rank for the uplink. This is an important contrast to purely temporal models, where flat fading in the downlink also implies flat fading in the uplink.

3 Basic modelling

In general, the angle-dependent complex impulse response of a mobile communications channel can be divided into four parts as

$$h(t,\tau,\varphi) = h_{LOS}(t,\tau,\varphi) + h_{MS}(t,\tau,\varphi) + h_{distant}(t,\tau,\varphi) + h_{BS}(t,\tau,\varphi) \quad (3)$$

where t the absolute time, τ is the delay, h_{Los} the impulse response associated with the LOS path, h_{MS} the impulse response due to scatterers in the vicinity of the MS; h_{BS} represents the contributions of scatterers near the base station, and $h_{distant}$ is the impulse response due to distant scatterers and/or reflectors. Although the scatterers close to the BS may be regarded in principle as acting in cascade with the other three propagation mechanisms, we treat them here as parallel mechanisms for simplicity. Conventional models have dealt with the angle-integrated impulse response, i.e. modelled the distribution of $p_{LOS,MS,distant,BS}(t, \tau)$. For performance assessment of mobile communication systems with smart antennas, however, the directional distributions $p_{LOS,MS,distant,BS}(\varphi)$ of the different contributions to the impulse response are essential.

If we know (or assume) the locations (i.e. spatial distribution) of the L scatterers, we can compute the impulse response at the BS as

$$h(t,\tau,\varphi) = \sum_{l=1}^{L} g_l(t,\varphi)\delta(\tau - \tau_l) \quad (4)$$

where δ is the Dirac delta function. The path amplitude $g_l(t, \varphi)$ follows as (Fig. 1)

$$g_l(t,\varphi) = (r_l^{(m)} \otimes r_l^{(M)})^{-\alpha/2} a_l \exp(j\phi_l)\delta(\varphi - \varphi_{l,BS}) \times \exp\left(-j\frac{2\pi}{\lambda} v_M \cos(\varphi_{l,MS} - \varphi_{v_{MS}})t\right) \times \exp\left(-j\frac{2\pi}{\lambda}\left(r_l^{(m)} + r_l^{(M)}\right)\right) \quad (5)$$

and

$$\tau_l = \frac{r_l^{(m)} + r_l^{(M)}}{c_0} \quad (6)$$

where $r_l^{(M)}$ and $r_l^{(m)}$ denote the distance from the mobile to the lth scatterer and the distance from the lth scatterer to the mth antenna element of the BS, respectively. For the BS (MS) the lth scattering point appears under the azimuth angle $\varphi_{l,BS}$ ($\varphi_{l,MS}$) and is characterised by a scattering coefficient $a_l e^{j\phi l}$. Strictly speaking, the angle $\varphi_{l,BS}$ depends also on the location of the mth antenna element. However, if we assume that the scattering points are in the far field of the BS antenna, this dependence can be neglected. The mobile is assumed to have a velocity $\vec{v}_{MS}$ so that $r_l^{(M)}$ varies with the absolute time t. $\varphi_{v_{MS}}$ is the azimuth angle of the velocity vector $\vec{v}_{MS}$, α denotes the power attenuation exponent, f_0 is the carrier frequency and c_0 is the velocity of light. In eqn. 5 the symbol $r_l^{(m)} \otimes r_l^{(M)}$ denotes $r_l^{(m)} \cdot r_l^{(M)}$ for scattering and $r_l^{(M)} + r_l^{(m)}$ for specular reflections. The location of the scatterers is discussed subsequently. The position of the MS is assumed to be uniformly distributed in the cell area, which is an annular region $r_1 < r_{MS} < r_2$.

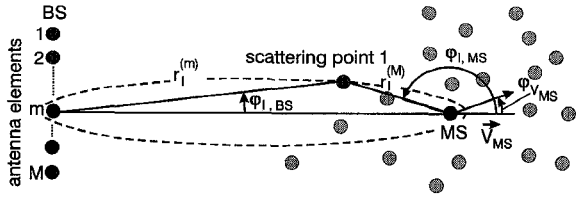

Fig. 1 *Propagation scenario where lth of (many) paths linking mth antenna element of base station BS and mobile station MS is highlighted*

3.1 Line-of-sight components

In mobile communications we can have LOS, quasi-LOS, or obstructed LOS between BS and MS, and the presence of this LOS component may change with time. To incorporate an LOS path with its associated behaviour over time, a propagation path with impulse response h_{LOS} for the direct connection between MS and BS is assigned

$$h_{LOS}(\tau,t,\varphi) = g_{LOS}(t)\delta(\tau - \tau_{min})\delta(\varphi - \varphi_0) \quad (7)$$

where τ_{min} is the delay time associated with the LOS connection. This propagation path is subject to shadowing. Usually its amplitude $|g_{LOS}(t)|$ is distributed log-normally. A typical model for the correlation function of the amplitude in dB is an exponentially decreasing correlation function [15]. The arriving LOS power is higher by the Rice factor K_{Rice} than the small-scale fading contributions.

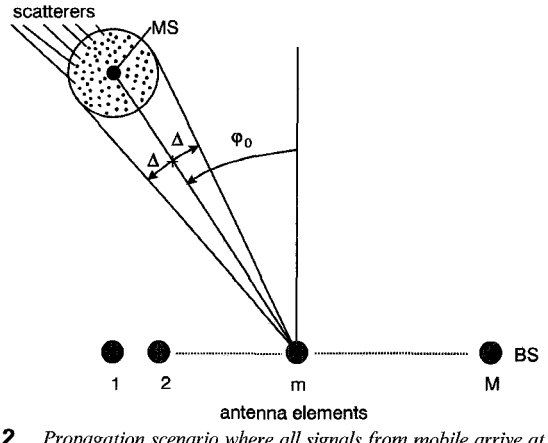

Fig. 2 *Propagation scenario where all signals from mobile arrive at base station in interval [– Δ, + Δ] centred around φ_0*

3.2 Local scatterer model

The local scatterer model describes the component $h_{BS}(t, \tau, \varphi)$ or $h_{MS}(t, \tau, \varphi)$ in eqn. 3. The azimuthal power spectrum (APS) for a BS antenna above rooftop is not discrete in rural and suburban mobile radio [1, 5, 16]. (Strictly speaking, APS is a spectral density; however, for ease of notation, we call it a 'spectrum'.) Rather, it consists of a nominal DOA associated with an angular spread. This can be explained by the fact that, in these environments, the BS antenna has typically LOS to the vicinity of the mobile. Thus, the local scattering around the mobile generates signals that arrive mainly within a certain angular range at the BS antenna. Fig. 2 shows a typical scenario, where the sig-

nals from the mobile arrive at the BS within an interval $[-\Delta, \Delta]$, centred at φ_0. The local scattering model was also analysed in [1, 17, 18], where theoretical and experimental results show the relationship between the DOA and beamwidth and the correlation of the fading between different antennas.

3.2.1 Spatial distribution of scatterers: A simple model of the spatial probability density function (PDF) of the scatterers around the mobile station is

$$p_1(\vec{r}) = \begin{cases} \frac{1}{R^2\pi} & \|\vec{r} - \vec{r}_{MS}\| \leq R \\ 0 & \text{elsewhere} \end{cases} \quad (8)$$

where $\vec{r}$ is the location vector taking the BS position as the origin, R is the radius of the scatterer circle, and $\vec{r}_{MS}$ is the location vector of the MS with respect to the BS position. Lee [19] suggested a radius of the local scattering circle (not a disc!) of 100 to 200λ. At the frequency of 800MHz, this translates to 40 to 80m. The measurements of [20, 21] at 1800MHz suggest a local scattering disc of radius approximately 100m. We conclude that in the UHF range this radius is more dependent on the environment than on wavelength as implied by Lee's formulation. (A certain wavelength dependence, smaller than linear, will remain because more remote scatterers are more easily shadowed at small wavelength, which renders them ineffective.) However, relevant scatterers are more likely to be close to the MS, and their number does not drop as sharply as in the preceding model. A Gaussian distribution

$$p_2(\vec{r}) = \frac{1}{2\pi R^2} \exp\left[-\frac{\|\vec{r} - \vec{r}_{MS}\|^2}{2R^2}\right] \quad (9)$$

is a better approximation to physical reality. Note that $\vec{r}$ is a position vector and not a scalar distance.

From the spatial distribution of the scatterers we can compute the APS by geometrical considerations [22, 23]. A uniform spatial distribution of scatterers does not lead to a uniform distribution of the DOAs in the range $-\Delta < \varphi < \Delta$. Actually, distributions of scatterers that lead to a uniform distribution of DOAs are difficult to justify physically. Nevertheless, this DOA distribution is widely used.

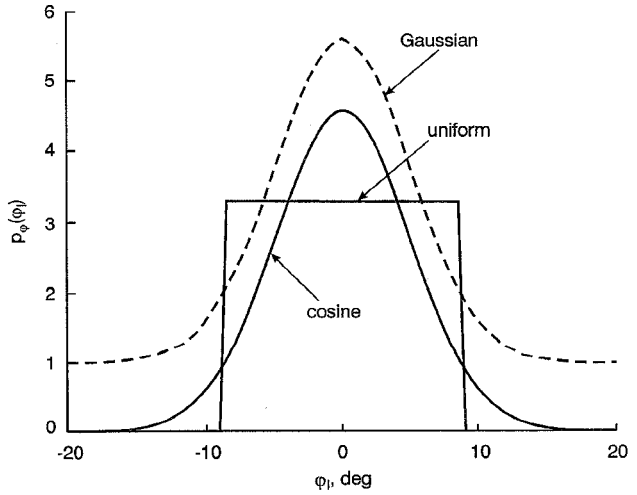

Fig.3 *APSs of incident signals for angular spread of $S_\varphi = 5°$*
Curve for Gaussian PDF is shifted by '1' in the ordinate, otherwise it would be masked by cosine-shaped PDF

3.2.2 Azimuthal power spectrum: Depending on the spatial distribution of the scatterers, different PDFs for the azimuth distribution of the incident waves as seen from the BS have been proposed in the literature. [1] proposed a $\cos^n(\varphi)$ function, [18] used a uniform distribution of the DOAs around the mean DOA, and [17] proposed a truncated normal distribution, i.e.

$$p_\varphi(\varphi_l) = \frac{Q}{\sqrt{2\pi\sigma_\varphi^2}} \exp\left[-\frac{(\varphi_l - \varphi_0)^2}{2\sigma_\varphi^2}\right]$$
$$\text{for } -\pi/2 + \varphi_0 \leq \varphi_l \leq \pi/2 + \varphi_0 \quad (10)$$

where σ_φ is the standard deviation of the APS and Q is a normalisation constant making $p_\varphi(\varphi_l)$ a PDF. The three functions are shown in Fig. 3 for an angular spread of $S_\varphi = 5°$. The curve for the Gaussian PDF is shifted by '1' in the ordinate; otherwise it would be masked by the cosine-shaped PDF. The cosine-shaped PDF is essentially the same as the Gaussian PDF. This is important because the Gaussian PDF allows closed-form computation of, e.g. the angular spread or the correlation function, while for the $\cos^n$ distribution numerical evaluation is inevitable. (Theoretically, a closed-form computation is possible also here but requires a series with n terms; since n is typically on the order of 100, this is not practical.) The angular spread S_φ [6] is determined as

$$S_\varphi = \begin{cases} \Delta/\sqrt{3} & \text{uniform PDF} \\ \sigma_\varphi\sqrt{Q\,\text{erf}\left(\frac{\pi}{\sqrt{8}\sigma_\varphi}\right)} & \text{Gaussian PDF} \end{cases} \quad (11)$$

where $\text{erf}(a)$ is the real-valued error function. Recent measurements [21] have shown that a Laplacian distribution of the APS can occur in practice; this distribution is given as

$$p_\varphi(\varphi_l) = \frac{Q_L}{\sqrt{2\sigma_\varphi^2}} \exp\left[-\frac{\sqrt{2}|\varphi_l - \varphi_0|}{\sigma_\varphi}\right]$$
$$\text{for } -\pi/2 + \varphi_0 \leq \varphi_l \leq \pi/2 + \varphi_0 \quad (12)$$

where again σ_φ is the standard deviation of the APS and Q_L is a normalisation constant. The angular spread follows as

$$S_\varphi = \frac{Q_L}{\sqrt{2\sigma_\varphi^2}}\left[\sqrt{2}\sigma_\varphi^3 - \frac{1}{4}\exp\left(-\frac{\pi}{\sqrt{2\sigma_\varphi^2}}\right) \times (\pi^2 + 4\sigma_\varphi^2 + \sqrt{8}\pi\sigma_\varphi)\right] \quad (13)$$

3.2.3 Correlation coefficients: The envelope correlation coefficient ρ_{env} of the signals received by two antennas spaced by d at the BS can be calculated in closed form for the Gaussian PDF by analogy to [18]. $\rho_{real}(d)$, the correlation coefficient between the real parts of the two signals (or the correlation between the imaginary parts) follows as [13]

$$\rho_{real}(d) = J_0\left(\frac{2\pi}{\lambda}d\right) + Q\sum_{k=1}^{\infty} J_{2k}\left(\frac{2\pi}{\lambda}d\right) \times \exp\left[-\frac{\sigma_\varphi^2(2k)^2}{2}\right][\cos(2k\varphi_0)\mathcal{A}(2k, \sigma_\varphi) - \sin(2k\varphi_0)\mathcal{B}(2k, \sigma_\varphi)] \quad (14)$$

and $\rho_{imag}(d)$, the correlation coefficient between the real and the imaginary parts of the two signals,

follows as

$$\rho_{imag}(d) = Q\sum_{k=1}^{\infty} J_{2k+1}\left(\frac{2\pi}{\lambda}d\right)\exp\left[-\frac{\sigma_\varphi^2(2k+1)^2}{2}\right] \times [\cos((2k+1)\varphi_0)\mathcal{A}(2k+1,\sigma_\varphi) + \sin((2k+1)\varphi_0)\mathcal{B}(2k+1,\sigma_\varphi)] \quad (15)$$

The $J_k(\cdot)$ are the Bessel functions of first kind and integer order. The quantities $\mathcal{A}(a, b)$ and $\mathcal{B}(a, b)$ are

$$\mathcal{A}(a,b) = \mathrm{Re}\left\{\mathrm{erf}\left(\frac{\pi}{\sqrt{8}b} - j\frac{ab}{\sqrt{2}}\right)\right\} - \mathrm{Re}\left\{\mathrm{erf}\left(-\frac{\pi}{\sqrt{8}b} - j\frac{ab}{\sqrt{2}}\right)\right\} \quad (16)$$

and

$$\mathcal{B}(a,b) = \mathrm{Im}\left\{\mathrm{erf}\left(\frac{\pi}{\sqrt{8}b} - j\frac{ab}{\sqrt{2}}\right)\right\} - \mathrm{Im}\left\{\mathrm{erf}\left(-\frac{\pi}{\sqrt{8}b} - j\frac{ab}{\sqrt{2}}\right)\right\} \quad (17)$$

where erf(a + jb) is the complex-valued error function [24]. Both tabulated values [24] and a polynomial approximation [25] are available. The envelope correlation coefficient ρ_{env} follows from the results as [1]

$$\rho_{env} = \frac{\mathcal{E}\{x_1x_2\}^2 + \mathcal{E}\{x_1y_2\}^2}{\mathcal{E}\{x_1^2\}^2} = \rho_{real}^2 + \rho_{imag}^2 \quad (18)$$

where $\mathcal{E}\{\cdot\}$ denotes expectation over location (space), $x_1(x_2)$ is the real value of the complex-valued signal at antenna element 1 (2), y_1 (y_2) is the imaginary part of the signal at antenna element 1 (2), and the squares indicate that one considers powers. Figs. 4–6 show the envelope correlation coefficient ρ_{env} for various mean angles of incidence φ_0 and angular spreads S_φ. The correlation coefficient decreases with increasing angular spread and with decreasing angle of incidence of the signals from broadside. The largest correlation is achieved at φ_0, = ±90° and S_φ = 0°. The consequences of this behaviour of the correlation coefficient are twofold:

- If the angular spread is rather small, the output signals of the elements of the BS antenna array are strongly correlated. This enables the application of techniques to determine the DOA from the knowledge of the array structure alone – so-called spatial reference (SR) techniques (e.g. Unitary ESPRIT [28]). However, if the first antenna element is in a fading dip, all others will be in the same dip too. Therefore the array provides no diversity gain at all in this situation.

- If the angular spread of a closed area is rather large, there exist no discrete-valued DOAs and the signals of the different elements of a BS antenna array are only weakly correlated. The determination of DOAs is impossible (in fact, DOAs are nonexistent) but the signals can be combined by using maximal ratio combining (MRC). The antenna is effective as a diversity arrangement.

The frequency correlation function (which is important for uplink–downlink considerations) for a (spatially) uniform distribution of scatterers follows as [13]

$$\rho_{\Delta\omega} = \left[\frac{2c_0}{R\Delta\omega}J_1\left(\frac{\Delta\omega R}{c_0}\right)\right]^2$$

and for the Gaussian PDF as

$$\rho_{\Delta\omega} = \exp\left[-\left(\frac{R\Delta\omega}{\sqrt{2}c_0}\right)^4\right] \quad (19)$$

where $\Delta\omega$ is the frequency offset. Fig. 7 shows the frequency correlation $\rho_{\Delta\omega}$ for different radii R of the scattering disc. The correlation increases with decreasing R. The fading of two signals at different frequencies can be considered as 'uncorrelated' if $\rho_{\Delta\omega} \leq 0.5$. For a scattering disc with $R = 100\lambda$ and uniform PDF, the fading of two signals is uncorrelated if they are separated by at least 0.26% (0.14%) of the centre frequency. This agrees very well with the lower bound for the coherence bandwidth obtained by applying Fleury's uncertainty theorem [26].

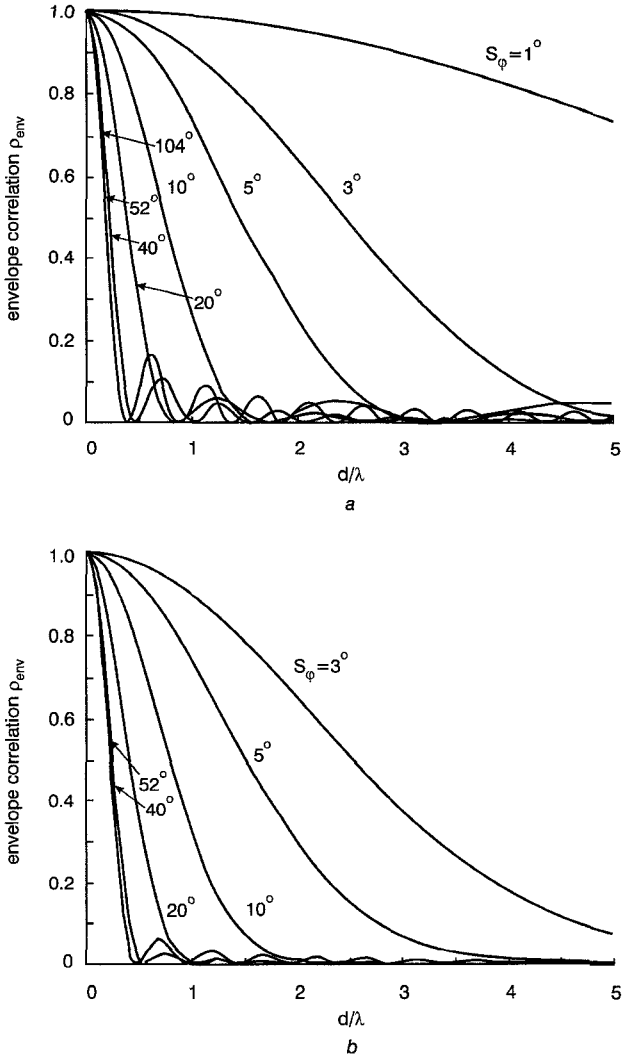

Fig. 4 *Envelope correlation coefficient for angle of incidence φ_0 = 0 against distance of antennas with angular spread S_φ as parameter*
a Uniform APS
b Gaussian APS

3.3 Distant scatterers

In both urban and rural environments, there are large structures that act as strong scatterers even if they are far away from both the base and the mobile stations. Examples of such structures are mountains, skyscrapers, buildings with metallised windows, monuments, etc. If these structures have LOS to both the BS and the MS, they can act as discrete reflectors or as clustered scatterers. In the former case, $h_{distant}(t, \tau, \varphi) \propto \delta(\tau - \tau_{distant})\delta(\varphi - \varphi_{distant})$. In the latter case, the BS sees a cluster of scattered components just as in the local scat-

tering model. An example for such geometries and their associated impulse response is shown in Fig. 8.

A different situation can occur if the BS has LOS to the scatterer, but the MS does not, e.g. if the wave propagating from the scatterer to the MS is guided by a street canyon. The APS is then mainly determined by the width of the street canyon (similarly to a microcell, see later). Such a situation can occur quite often in urban areas, as evidenced by measurements [27].

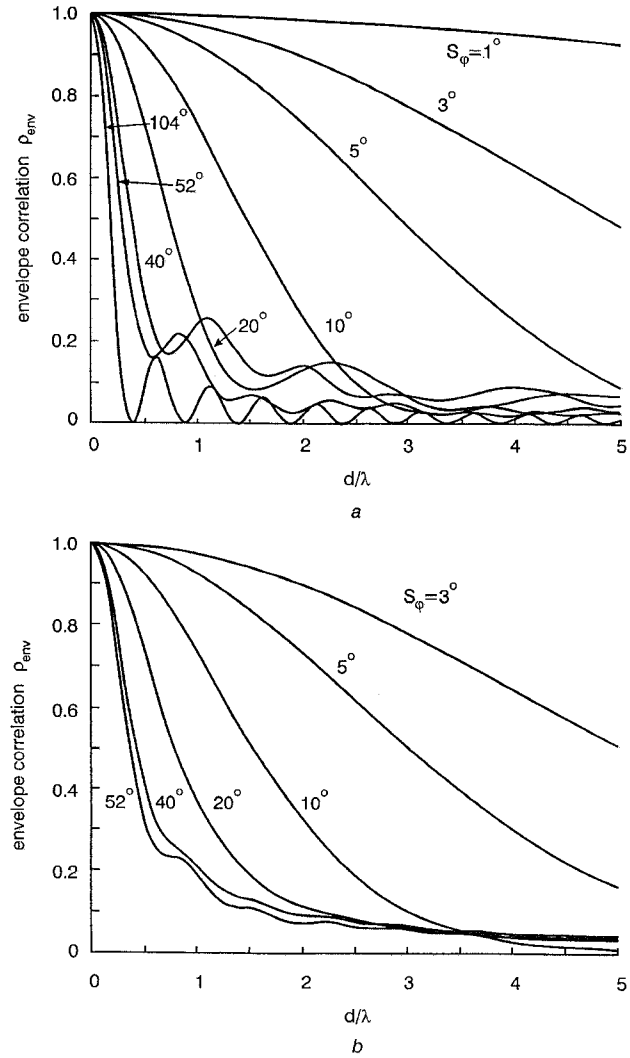

Fig. 5 *Envelope correlation for angle of incidence φ_0 = 60° against distance of antennas with angular spread S_φ as parameter*
a Uniform APS
b Gaussian APS

3.4 Base station scatterers

As can be seen from eqn. 3, scatterers around the base station also can play a role. For these scatterers, the same spatial distribution (i.e. uniform or Gaussian) is assumed as for the MS. However, the APS is different. The DOAs are now uniformly distributed in $0 < \varphi < 2\pi$ (as seen from the BS; of course, the MS sees these scatterers in a small angular range). These scatterers play an important role in micro- or picocells only, when the BS is below rooftop level.

4 Low-rank channel models

Fig. 9 gives an overview of our proposal for low-rank channel models. A low-rank channel model requires that contributions from scatterers around the base station and from distant scatterers are negligible. It basically consists of the local scattering model around the MS associated with a LOS component. The parameters for these models are summarised in Table 1. The range for the radius of the scattering disc is somewhere within 50 to 300m (Section 3.2.1) and the maximum cell radius is the maximum radius of a macrocell for the considered system (say, GSM). The APSs are to be interpreted as mean values of the incident power against angle, i.e. they are averaged over a large number of instantaneous spectra.

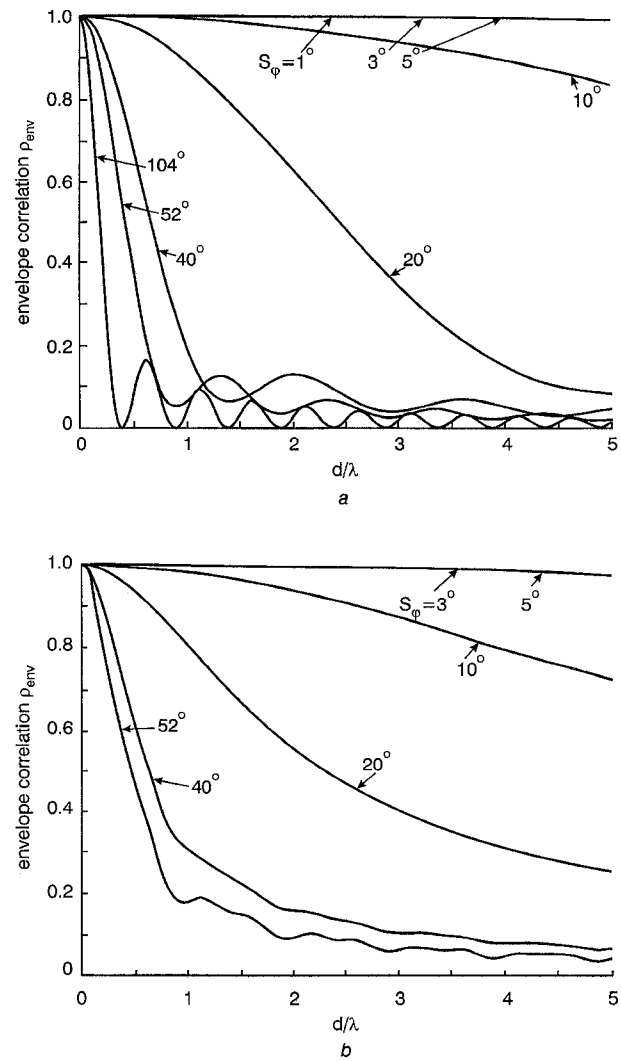

Fig. 6 *Envelope correlation for angle of incidence φ_0 = 90° against distance of antennas with angular spread S_φ as parameter*
a Uniform APS
b Gaussian APS

One might wonder why the azimuthal dispersion has to be specified even if the channel is low-rank, i.e. the angular distribution cannot be resolved by the antenna main lobe. The answer is twofold: (i) DOA estimation algorithms can determine angles of arrival with an accuracy that is much higher than the beamwidth of the antenna. The actual resolution accuracy is mainly limited by the angular spread around the mean direction of arrival and the signal-to-noise ratio. (ii) In smart antenna systems, we are mainly interested in putting antenna pattern nulls on interferers. The nulls are much sharper than the main lobes, and the amount of residual interference is critically determined by the product of the antenna pattern near the null and the APS around the direction of the interferer.

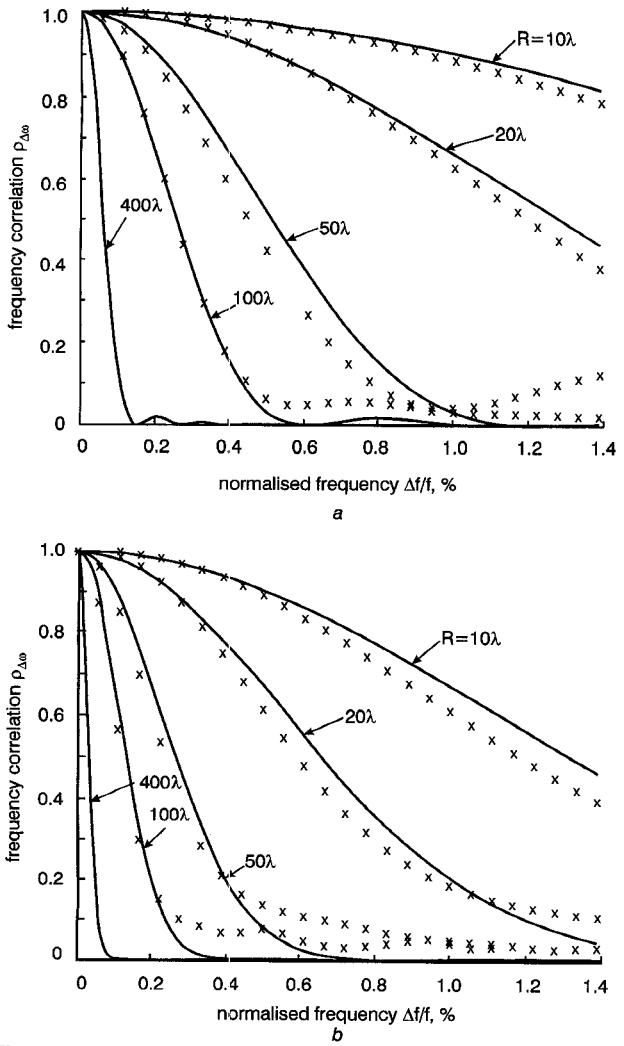

Fig. 7 *Frequency correlation against normalised frequency separation $\Delta f/f_0$ with radius R of scattering circle as parameter*
——— theory; × simulations
a Uniform PDF for scatterers around MS
b Gaussian PDF for scatterers around MS

5 High-rank channel models

In environments with large delay spreads and/or large angular spreads we cannot use low-rank models. High-rank channel models taking into account local scattering and distant scatterers are needed. We propose two ways of generating high-rank channel models:

- **Addition of distant scatterers**: Add distant scatterers (where each can be either a discrete reflector or can consist of a disc of scatterers) to achieve large delay and angular spreads. An example is given in Fig. 8. Here, two discs with scatterers give rise to time dispersion and to a large angular spread. The parameters for the local scattering model given in Table 1 also form the basis for the high-rank channel models.

- **Heavy scattering around the BS**: We considered two possible ways of modelling local scattering around the BS:

- A scatterer disk around the BS antenna. This is most appropriate for microcells, where the antennas are located below rooftop level. There are local scatterers both close to the MS and to the BS antenna.

- A scattering region may encompass both BS and MS, as it is most likely for picocells and short-range indoor wireless communications.

Fig. 10 gives an overview of the appropriate scattering models for the different cell types. The parameters for the channel models are listed in Table 2.

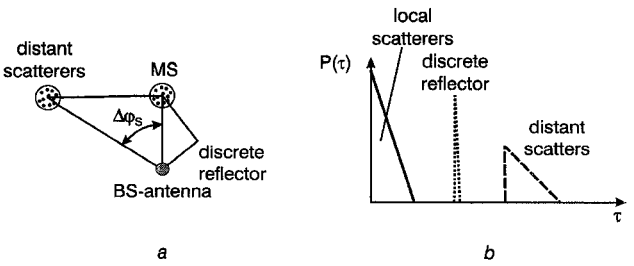

Fig. 8 *High-rank channel model example*
Local scatterers, distant scatterers and discrete reflector exist. PDS clearly reveals different contributions
a Physical channel model
b Power delay profile

5.1 Macrocells

The model for macrocells is usually a combination of local scattering with distant scatterer clusters (typically one) and distant discrete reflectors. This yields agreement with the COST 207 model [29] if we compute the Doppler spectra from the APS. The angle between the

Table 1: Parameters for local scattering model

Property	Dimensions	Comment
Radius R of local scattering circle (for BS & MS)	$50\,m \le R \le 300\,m$	see text
Number N_s of local scatterers	$N_s \ge 10$	ensures 'Rayleigh-statistic' of envelope
PDF of the angle φ_{scat} of local scatterers	$p(\varphi_{scat}) = 1/(2\pi)$ $0 < \varphi_{scat} \le 2\pi$	scatterers are all around BS or MS
Spatial PDF	$p_1(\vec{r}) = 1/(R^2\pi)$ $\|\| \vec{r} - \vec{r}_{MS} \|\| \le R$	[2]
	$p_2(\vec{r}) = (1/(2\pi R^2))\exp(-\|\| \vec{r} - \vec{r}_{MS} \|\|^2/(2R^2))$	our suggestion
Damping factor of local scatterer a_l	$p(a_l)$ uniform between [0, 1]	simplest physically reasonable distribution
PDF of phase shifts ϕ_l introduced by local scatterers	$p(\phi_l) = 1/(2\pi)$ $0 < \phi_l \le 2\pi$	[30]
Inner cell radius r_1	$r_1 \ge R$	definition of local scatterers
Outer cell radius r_2	$r_2 \le$ maximum system cell radius	definition of cell radius
PDF of distance r_{MS} between BS and MS	$p(r_{MS}) = 2r_{MS}/(r_2^2 - r_1^2)$ $r_1 \le r_{MS} \le r_2$	equal probability of MS location per unit area
Power in LOS-component	$K_{Rice} = 0 - 50$	[32]
Fading statistic of LOS-component g_{LOS}	log-normal, $\sigma = 5 - 12$ dB	[31]
Time behaviour of fading	exponential correlation model	[15]

Table 2: Parameters for high-rank channel models

Property	Dimensions	Comment
Microcells		
Parameters for local scattering models	as for low-rank channels	
Number N_{sd} of scatterer discs (MS plus distant)	$N_{sd} = 2$	[2]
PDF of angular distance $\Delta\varphi_s$ between two scattering scenarios	$p(\Delta\varphi_s) = 1/(q_1 - q_2)$ $0 \le q_2 < q_1 \le \pi$	arbitrary distribution
Number N_{discr} of discrete reflectors	$0 \le N_{discr} \le 4$	dependent on environment
PDF of angle $\varphi_{l,BS}$ of local scatterers at BS	$p(\varphi_{l,BS}) = 1/2\pi$) $0 < \varphi_{l,BS} \le 2\pi$	scatterers are all around BS
Power of local scatterers around BS	(30 ÷ 50) dB below power of scatterers around MS	[5]
Microcells		
Radius R of local scattering scenario	$R = w_{Street}/2$	geometry
Number N_s of scatterers	$N_s \ge 10$	see Table 1
Inner cell radius	$r_1 \ge 5$m	geometry
Outer cell radius	$r_2 \le 3000\lambda$	max. microcell radius
APS $p(\varphi_l)$	$p(\varphi_l) = k_1/i$ if $0 < \| \varphi_l - \varphi_i \| \le \pi/S_m$ $p(\varphi_l) = k_2$ elsewhere $S_m = 16$, $\varphi_i = \pm (2i - 1)2\pi/S_m$, $1 \le s \le S_m/2$ $i = 1, ..., s$; $k_2 = 0.0316$; $\Sigma_s = \Sigma_{i=1}^{s} 1/i$; $k_1 = S_m/(2\Sigma_s)(1/(2\pi)) - k_2(1 - 2s/S_m))$	stepwise approximation of APS
PDF of angle $\varphi_{l,BS}$ of local scatterers at BS	$p(\varphi_{l,BS}) = 1/(2\pi)$ $0 < \varphi_{l,BS} \le 2\pi$	see Table 1
Power of local scatterers around BS	(20 ÷ 40) dB below power of scatterers around MS	[5]
Picocells		
Radius of local scattering scenario	R = $w_{Room}/2$	geometry
Number of N_s of scatterers	$N_s \ge 10$	see Table 1
Inner cell radius	$r_1 \ge 0.3$m	geometry
Outer cell radius	$r_2 \le 50$m – 200m	typ. picocell radius
APS $p(\varphi_l)$	$p(\varphi_l) = k_1 \cos(k_2 \varphi_l)$, $-\pi \le \varphi_l \le \pi$ $k_1 = 0.2103$, $k_2 = 0.4$	approximation of APS with a sin(•)–function
PDF of angle $\varphi_{l,BS}$ of local scatterers at BS	$p(\varphi_{l,BS}) = 1/(2\pi)$ $0 < \varphi_{l,BS} \le 2\pi$	see Table 1
Power of local scatterers around BS	(0 ÷ 10) dB below power of scatterers around MS	[5]

scatterer clusters can be chosen arbitrarily.The distances are chosen according to the distribution functions for the local scattering model. In doing so, the delay has to be monitored to obtain models consistent with the COST 207 models. For example, for the bad urban area the delay of the second component (with respect to the first) should be around 5μs and for the hilly terrain the delay should be around 15μs. In addition, discrete components can be incorporated into the APS. This is important for urban areas with high-rise buildings. Even a single local-scattering model may result in a high-rank model if the BS is close to the MS, since the angular spread might be larger than the 3dB beamwidth of the antenna pattern.

The general parameters for the configuration of the model are given in Table 2.

5.2 Microcells

Microcells are characterised by antennas located below rooftop level. This means that scattering around the BS cannot be neglected. Additionally, the distances r_{MS} between BS and MS are typically an order of magnitude less than for macrocells. Because of the antenna height, the DOAs are mostly centred around the directions of the streets in the vicinity of the BS. The diameter of the local scatterer disc is mainly determined by the width of the streets w_{Street}. NLOS microcells can be characterised by scattering scenarios at the street crossings that have LOS to the BS; from these crossings the waves are guided to the MS. The APS is more uniform than for macrocells. The parameters of the model are summarised in Table 2.

5.3 Picocells

In picocells the APS can become almost isotropic [5, 16] when there is no LOS. The scattering circle usually encompasses both MS and BS owing to the small distances between BS and MS. If there is a LOS component the APS is of course biased into its direction, but the angular spread is larger than for any other environment [5]. The model parameters are given in Table 2.

6 Fixed- and moving-MS models

6.1 Fixed-MS model

For most system simulations it is sufficient to know the APS and the PDS (power delay spectrum) of the inci-

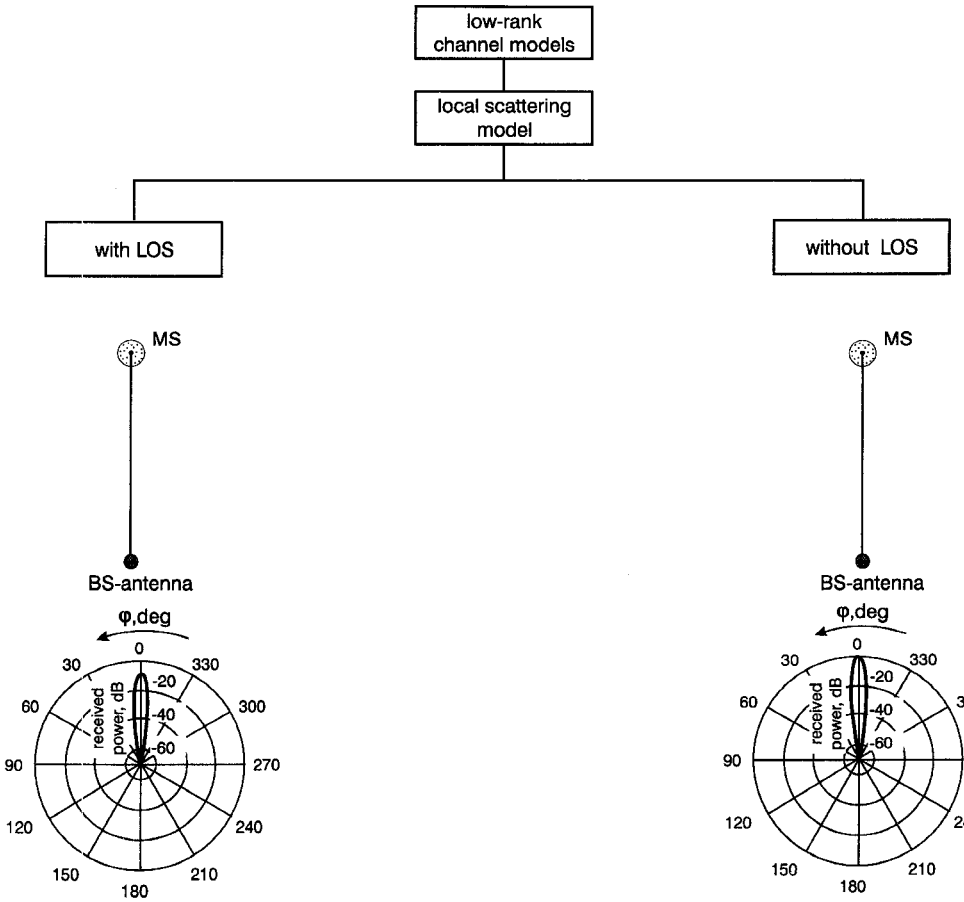

Fig. 9 *Channel models for low-rank channels*

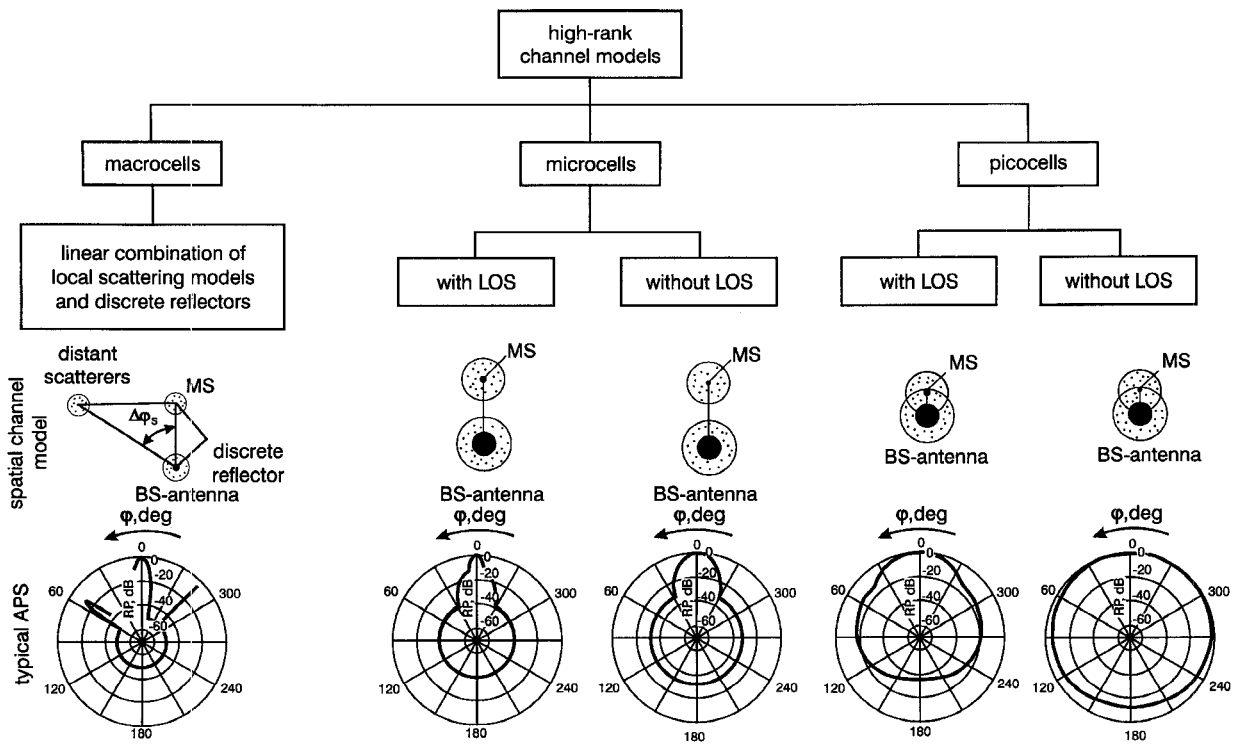

Fig. 10 *Channel models for high-rank channels*
RP = received power

dent field, independent of what these spectra were at earlier instants (e.g. for simulation of the uplink in smart antenna systems). In that case, one can either compute a distribution of N scatterers anew for each 'time instant' (i.e. each simulation run in a Monte Carlo simulation), or one can just choose the appropriate PDFs (APS and PDS), and select the instantaneous values at random from these PDFs; the latter approach is computationally more efficient. The APS can be computed from the models described in Sections 4 and 5 in conjunction with the parameters given in Tables 1 and 2.

6.2 Moving-MS model

There are some situations where we need to know the temporal evolution of the distribution of scatterers, e.g. when we analyse tracking algorithms for smart antenna systems. In that case the distribution of scatterers will change, albeit slowly, as the MS moves through the environment. Some local scatterers get out of range and some new local scatterers will appear. The appropriate model to take this effect into account is the moving MS model. Its principle is given by the following algorithm:

(i) For the instant $t = t_1$, place N scatterers around the location $\vec{r}_{MS,1} = [x_{MS}, y_{MS}]^T$ of the MS according to eqn. 8. (N is kept constant during the simulation.)

(ii) At the instant t_2 the MS has moved to the position $\vec{r}_{MS,2} = \vec{r}_{MS,1} + [v_{MS,x}, v_{MS,y}]^T (t_2 - t_1)$.

(iii) Define a new scatterer disc with its centre at the new location $\vec{r}_{MS,2}$ of the MS. Remove all scatterers outside the new scatterer disc. Their number be N_1.

(iv) If $N_1 = 0$ go back to step (ii) for the next instant.

(v) If $N_1 > 0$, new scatterers are generated within the new scattering area in accordance with the PDF of eqn. 8. The N_1 scatterers in the sickle-shaped region belonging to the new scatterer disc only are added to the model (Fig. 11). Go back to step (ii).

This selection procedure is necessary since just selecting N_1 new scatterers would bias the distribution of the scatterers towards the regions where the MS has been at earlier times. Transitions occurring when scatterers 'arrive' and 'vanish' are modelled as discrete events, although the transitions will be smooth in reality. Since, in our model, typically $N_1 << N$, the 'nonsmoothness' will not be very pronounced.

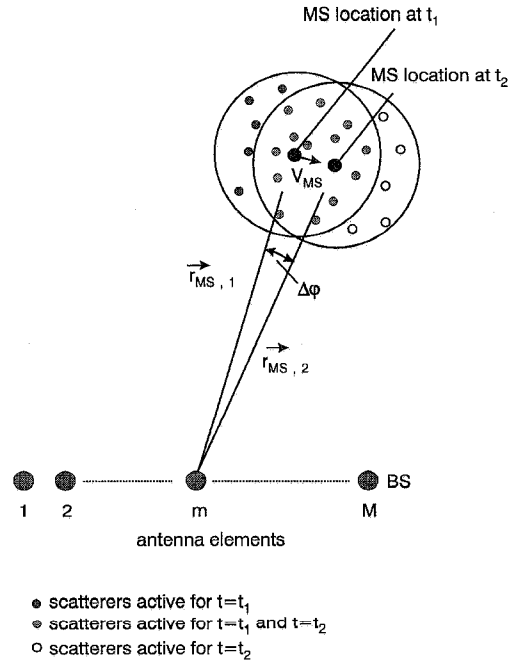

Fig. 11 *Principle of moving MS model showing two consecutive instants t_1 and t_2*
$N_1 = 6$ scatterers active at t_1 are outside scatterer circle at t_2. These are removed and $N_1 = 6$ new scatterers added.

7 Summary and conclusions

We have presented a unified modelling approach for mobile radio channels including DOAs. The models are based on prescribing a distribution of scatterers around the MS and BS. LOS components and distant discrete (or distributed) scatterers can be taken into account. By appropriately combining these contributions, all practically important situations (macro-, micro- and picocells, LOS and NLOS, static or moving MS) can be efficiently simulated. Furthermore, space-correlation coefficients and frequency-correlation coefficients can be calculated for these models. Tables 1 and 2 provide all parameters that are needed for implementation of the models in system simulations. With our new model the performance of smart antenna systems in various situations can be assessed in a realistic and consistent manner, thus allowing improved system design and capacity considerations.

8 Acknowledgments

Support of this work by Post & Telekom Austria (PTA) is gratefully acknowledged. The views expressed are those of the authors and do not necessarily reflect the views within the PTA. The authors thank Prof. Walter Leeb, Alexander Kuchar, and Juha Laurila for stimulating discussions and critical reading of the manuscript. They are grateful to the anonymous reviewers for valuable suggestions that helped to improve the paper.

9 References

1 LEE, W.C.Y.: 'Effects on correlation between two mobile radio base-station antennas', *IEEE Trans.*, 1973, **COM–21**, (11), pp. 1214–1224
2 BLANZ, J.J., BAIER, P.W., and JUNG, P.: 'A flexibly configurable statistical channel model for mobile radio systems with directional diversity'. Proceedings of 2nd ITG-Fachtagung Mobile Kommunikation, Neu-Ulm, Germany, September 1995, pp. 93–100
3 LIBERTI, J.C., and RAPPAPORT, T.S.: 'A geometrically based model for line-of-sight multipath radio channels'. Proceedings of 46th IEEE conference on *Vehicular technology*, VTC'96, Atlanta, USA, April/May 1996, pp. 844–848
4 NORKLIT, O., and BACH ANDERSEN, J.: 'Mobile radio environments and adaptive arrays'. Proceedings of 4th international symposium on *Personal, indoor and mobile radio*, PIMRC '94, The Hague, Netherlands, 1994, pp. 725–728
5 EGGERS, P.C.F.: 'Angular dispersive mobile radio environments sensed by highly directive base station antennas'. Proceedings of 6th international symposium on *Personal, indoor and mobile radio communications*, PIMRC '95, Toronto, Canada, September 1995, pp. 522–526
6 EGGERS, P.C.F.: 'Angular-temporal domain analogies of the short-term mobile radio propagation channel at the base station'. Proceedings of 7th international symposium on *Personal, indoor and mobile radio communications*, PIMRC'96, Taipeh, ROC, October 1996, pp. 742–746
7 BLANZ, J.J., KLEIN, A., and MOHR, W.: 'Measurement based parameter adaptation of wideband spatial mobile radio channel models'. Proceedings of IEEE fourth international symposium on *Spread spectrum technology and applications* ISSSTA'96, Mainz, Germany, 22–25 September 1996, pp. 91–97
8 KLEIN, A., MOHR, W., THOMAS, R., WEBER, P., and WIRTH, B.: 'Direction-of-arrival of partial waves in wideband mobile radio channels for intelligent antenna concepts'. Proceedings of IEEE 46th conference on *Vehicular technology*, VTC '96, Atlanta, USA, April/May 1996, pp. 849–853
9 MARTIN, U., and GRIGAT, M.: 'A statistical simulation model for the directional mobile radio channel and its configuration'. Proceedings of IEEE international symposium on *Spread spectrum technology and applications*, ISSSTA '96, Mainz, Germany, 1996, pp. 86–90
10 FUHL, J., and MOLISCH, A.F.: 'Space domain equalisation for second and third generation mobile radio systems'. Proceedings of 2nd ITG-Fachtagung Mobile Kommunikation, Neu-Ulm, Germany, September 1995, pp. 85–92
11 FUHL, J., and BONEK, E.: 'A comparative analysis of adaptation schemes for smart antennas'. Proceedings of international conference on *Telecommunications*, ICT'96, Istanbul, Turkey, April 1996, pp. 427–432
12 FUHL, J., and MOLISCH, A.F.: 'Capacity enhancement and BER in a combined SDMA/TDMA system'. Proceedings of 46th IEEE conference on *Vehicular technology*, VTC'96, Atlanta, USA, May 1996, pp. 1481–1485

13 FUHL, J.: 'Smart antennas for second and third generation mobile communications systems'. PhD thesis, Technical University, Vienna, 1997
14 MOLISCH, A.F.: 'Statistical properties of the rms delay spread of mobile radio channels with independent Rayleigh-fading paths', *IEEE Trans. Veh. Technol.*, 1996, **45**, (1), pp. 201–205
15 GIANCRISTOFARO, D.: 'Correlation model for shadow fading in mobile radio channels', *Electron. Lett.*, 1996, **32**, (11), pp. 958–959
16 OTTERSTEN, B.: 'Array processing for wireless communications'. Proceedings of workshop on *Statistical signal and array processing*, Corfu, Greece, June 1996, pp. 466–473
17 ADACHI, F., FEENEY, M.T., WILLIAMSON, A.G., and PARSONS, J.D.: 'Crosscorrelation between the envelopes of 900MHz signals received at a mobile radio base station site', *IEE Proc. F*, 1986, **133**, (6), pp. 506–512
18 SALZ, J., and WINTERS, J.H.: 'Effect of fading correlation on adaptive arrays in digital mobile radio', *IEEE Trans. Veh. Technol.*, 1994, **43**, (4), pp. 1049–1057
19 LEE, W.C.Y.: 'Applying the intelligent cell concept to PCS', *IEEE Trans. Veh. Technol.*, 1994, **43**, (3), pp. 672–679
20 MARTIN, U.: 'A directional radio channel model for densely built-up urban area'. Proceedings of 2nd European conference on *Personal mobile communications*/3rd ITG-Fachtagung Mobile Kommunikation'97, Bonn, September 1997, pp. 237–244
21 PEDERSEN, K.I., MOGENSEN, P.E., and FLEURY, B.H.: 'Power azimuth spectrum in outdoor environments', *Electron. Lett.*, 1997, **33**, (18), pp. 1583–1584
22 NORKLIT, O.: 'Adaptive antennas in mobile communication'. PhD thesis, Aalborg University, 1996
23 PETRUS, P., REED, J., and RAPPAPORT, T.: 'Geometrically based statistical channel models for macrocellular mobile radio environment'. Proceedings of GLOBECOM 96, pp. 1197–1201
24 ABRAMOWITZ, M., STEGUN, I.A.: 'Handbook of mathematical functions' (Dover, New York, 1965)
25 HUMLICEK, J.: 'Optimized computation of the Voigt and complex probability functions', *J. Quant. Spectrosc. Radiat. Transfer*, 1982, **27**, (4), pp. 437–444
26 FLEURY, B.H.: 'An uncertainty relation for WSS processes and its application to WSSUS systems', *IEEE Trans. Commun.*, 1996, **44**, (12), pp. 1632–1634
27 FUHL, J., ROSSI, J.P., and BONEK, E.: 'High-resolution 3D direction-of-arrival determination for urban mobile radio channels', *IEEE Trans.*, 1997, **AP—45**, (4), pp. 672–682
28 HAARDT, M., and NOSSEK, J.A.: 'Unitary ESPRIT: How to obtain an increased estimation accuracy with reduced computational burden', *IEEE Trans. Signal Process.*, 1995, **43**, (5), pp. 1232–1242
29 Commission of the European Communities: 'Digital land mobile radio communications — COST207' ECSC–EEC–EAEC, Brussels, 1989
30 JAKES, W.C.: 'Microwave mobile communications' (IEEE Press, Piscataway, USA, 1974)
31 STUEBER, G.L.: 'Principles of mobile communication' (Kluwer, Dordrecht, The Netherlands, 1996)
32 BRAUN, W.R., and DERSCH, U.: 'A physical mobile radio channel model', *IEEE Trans. Veh. Technol.*, 1991, **40**, (2), pp. 472–482